Available online at www.sciencedirect.com

ScienceDirect

Procedia Structural Integrity 78 (2026) 591–598

Structural Integrity Procedia

www.elsevier.com/locate/procedia

XX ANIDIS Conference

Seismic performance and modelling of reinforced concrete frames infilled with sliding joint ductile infills

Simone Pelucco[a], Van Sang Doan[a], Simone Vincenzi[a], Marco Preti[a,*]

[a]*Department of Civil, Environmental, Architectural, Engineering and Mathematcis, University of Brescia, via Branze, 43, Brescia, 25123, Italy*

Abstract

The paper explores the seismic performance of reinforced concrete (RC) frames infilled with deformable masonry panels incorporating horizontal sliding joints. These innovative infill systems are designed to overcome the seismic vulnerabilities observed in traditional RC structures with rigid infills, where the interaction between the frame and infill often leads to undesirable brittle failure mechanisms. The study analyses the response of a 5-storey structure, adopted as a RC case study, varying the infill properties and layouts and the design ductility classes. The structural responses are assessed through linear, non-linear static and non-linear dynamic analyses, and they are discussed across different seismic performance limit states. Focus is on the ductility verification, collapse mechanisms and non-regularity in the infill distribution in elevation. Comparative results reveal how the presence of deformable infills under varying design parameters and different modelling strategies affects the global seismic response, and these results provide support to the development of design guidelines. Overall, the findings confirm the potential of sliding-joint infills in improving seismic performance and support their possible incorporation into performance-based design methodologies. The study also highlights the potential capability of Response Spectrum Analysis and Pushover analysis to capture the seismic demands in infilled frames.

Keywords: Ductile masonry infill; sliding joint; seismic resistant frame; earthquake damage mitigation; soft storey;

* Corresponding author.
E-mail address: marco.preti@unibs.it

10.1016/j.prostr.2025.12.076

1. Introduction

Reinforced concrete (RC) frames with traditional masonry infills have demonstrated their seismic vulnerability in several earthquake events (Braga et al., 2011, Fikri et al., 2019), due to the interaction between the infill and the frame. Starting from the idea of Langenbach, (2007) and the work of Mohammadi & Akrami, (2010), a family of deformable infills was developed, typically obtained by subdividing the wall into sliding subpanels (Preti et al., 2012) or by decoupling the infill from the frame using deformable joints along its perimeter (Ju et al., 2012). The peculiarity of such proposals is to both reduce the high shear action demand on the columns and the significant in-plane damage of the traditional interacting masonry infills, keeping the advantage of the use of masonry panels for acoustic and thermal performances. Research programs have focused on the role of infills in the structural frames during earthquakes, and design codes (Draft Eurocode 8) are progressively placing more emphasis on their proper design and the associated safety checks. Among the seismic-resilient solutions, ductile infills with sliding joints have been developed with the aim of controlling the detrimental effect of the infill-frame interaction, reducing post-earthquake damage and enabling a rational prediction of the building seismic response. Experimental (Morandi et al., 2018) and numerical (Bolis et al., 2017) studies have supported their potential with this regard, but guidelines are still needed to ensure their safe design and to properly proportion the structural frame in their presence. In particular, structural detailing for overstrength, behavior factor choices and criteria for the application of simplified methods of analysis of the infilled frame structure are required for their implementation in the design practice. Guidelines for mitigation of the detrimental effect of possible non regular infill distribution effect are required as well.

The paper describes a synthesis of the results of a parametric analysis aimed at supporting the upcoming required design guidelines. The analysis uses a 5-storey building case study designed according to the today Eurocodes and Italian building code. Following a widely adopted approach, infills are not explicitly included in the design model of the structure, but their effect is quantified in the detailed analysis of the structure seismic response. The reason for this approach lays in the non-structural function of the infills, which makes them susceptible to changes in the composition and layout during the building working life, due to possible building architectural renovation or change of destination. Therefore, their effects are taken into account on the structural safety checks, including the possible change in the infill layout, particularly focusing on the soft-storey mechanism. Three methods of seismic analyses of the structure are performed and compared, namely Linear dynamic response spectrum analysis (RSA), Non-linear static analysis (PO), Non-linear dynamic time-history analysis (NLTH). Three different levels of ductility and infill strength are explored, together with a non-regular distribution of infills in elevation.

2. Case study

The case study focuses on a residential building in the Municipality of Cosenza (CS), a high-seismicity area in Italy, designed with an RC moment-resisting frame structure. The site conditions include soil type “C” and topography category “T1”. The building consists of five spans in the primary (longitudinal) direction, three spans in the transverse direction, and a total of five floors (Fig. 1), founded on a rigid box underground structure. The design follows the Italian building code and the European seismic standard. The construction materials used are C35/45 concrete and B450C steel.

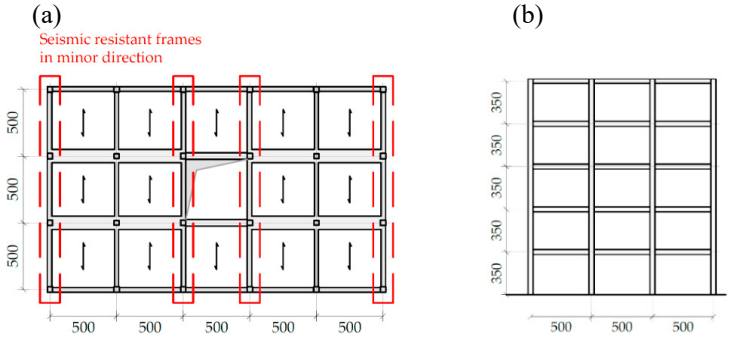

Fig. 1. The case study structure in plan (a) and elevation (b) focusing on the seismic resistant frame in the minor direction (dimensions in [mm])

The design gravity loads are reported in Table 1. Regarding the infills, they are located along the perimeter and on the two internal frames near the central opening. These frames stiffened by the infills are also considered primary elements, while the remaining frames are considered secondary elements and are designed for gravity loads only.

The case study frame will be focused on one of the two external frames aligned along the shorter building length.

The seismic design is carried out using a Response Spectrum Analysis (RSA), and the elastic response spectra for the construction site are shown in Fig. 2.

Table 1. Design gravity load.

Floor type	G1 (kN/m^2)	G2 (kN/m^2)	Q (kN/m^2)
Floors	3.55	3.60	2.00
Roof	3.55	3.30	0.50
Line loads			
Infills load (kN/m)	7.56		

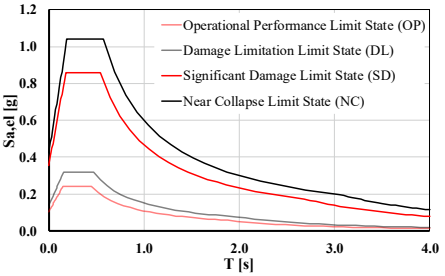

Fig. 2. Design horizontal acceleration elastic spectra

As mentioned, the design of the primary frame is performed neglecting the stiffening contribution of the non-structural elements, particularly of the infills. Precautions against the detrimental effect of the infilled frame interaction is taken according to the prescription included in the Eurocode 8 (2004) and the Italian NTC (2018). The case study bare frame is modelled using a bidimensional design, and this simplification is allowed by code as long as the bending strength of the columns is reduced to 70% (Eurocode 8 (2004)). This is to ensure the compliance with capacity design and hierarchy of strength principles in the tridimensional response, including bidirectional horizontal seismic excitation. Column cross section was kept constant in elevation. To account for concrete cracking, a uniform stiffness reduction factor of 0.5 is applied to all members during the design. At the Serviceability Limit States (SLS), the interstorey drift limits specified for ductile infill walls are considered, with values set as follows: δ_{DL} = 1.0 % and δ_{OP} = 2/3 δ_{DL}.

To explore the influence of ductility, three different ductility levels (namely “high” (DCH), “medium” (DCM), and “low” (DCL)) are considered in the design, resulting in three frames with different flexibility levels. The design behavior factors of each frame are reported in Table 2. The behavior factor in the DCH class design is reduced with respect to the maximum allowable, equal to 5.85, because at the fundamental period of the structure, the resulting spectrum is characterized by ordinates lower than the minimum spectral acceleration equal to $0.2a_g$ indicated by the Italian NTC at §3.2.3.5 and the European one at §3.2.2.5. The DCL frame is designed for a behavior factor equal to 2.7 to limit the plasticization both at the serviceability and ultimate limit states. Size and reinforcement of the structural element are optimized to match the minimum required design flexural strength in the plastic hinge sections of the assumed collapse mechanism, with a target 10% maximum nominal overstrength of the design resisting bending moment compared to the corresponding effect of actions.

The dynamic behavior of the frames is characterized by their fundamental periods, calculated for both uncracked and cracked section conditions. These results are reported in Table 2. As expected, the fundamental period increases with an increasing ductility level, due to the reduced cross-sections and consequent greater flexibility of the structure.

Table 2. Selected behaviour factors and fundamental periods of the different frame models: Uncracked sections with full elastic stiffness (“Uncracked”), cracked section with assumed 50% reduced stiffness for beams and columns (“Design”), and cracked section with assumed 30% and 50% reduced stiffness for beams and columns, respectively,(“Comparison”) for comparison to non-linear analysis types.

Ductility	α_I/α_u	q0	q	T_1 Uncracked	T_1 Design	T_1
DCH	1.3	5.85	5.85 → 4.9	1.27s	1.79s	2.09s
DCM	1.3	3.9	3.9	1.03s	1.46s	1.70s
DCL	N.A	N.A	2.7	0.79s	1.11s	1.29s

Note that the effective cracked stiffness of the beams (Paulay & Priestley, 1992), especially those subjected to low axial forces, is significantly reduced, to less than half of the uncracked section stiffness. To ensure consistency and reliability when comparing seismic demands from RSA and nonlinear analysis results, a stiffness reduction factor of 0.3 is adopted for the beams in the RSA analysis (Pelucco, 2024).

Each frame is examined in different configurations: bare, traditional and ductile infills (with three different infill thicknesses 200, 250, and 300 mm), including the case of lacking infill at the ground level. The mechanical and geometrical properties of the infills required for their modelling follow Preti et al. (2015) and Di Trapani et al. (2020).

3. Method of analysis

The case study structure response is analyzed and compared with three different methods of analysis: linear dynamic response spectrum analysis (RSA), non-linear push-over static analysis (PO) and non-linear time-history dynamic analysis (NLTH). The infills are explicitly modelled by means of concentric equivalent diagonal strut macro-models according to Preti et al. (2019) and Di Trapani et al. (2020). The column shear overload induced by the trust of the infill on the columns is quantified a posteriori. The infill macro-model is calibrated with an axial constitutive law to reproduce the reaction of the infill to the bay sway mechanism.

In terms of the ductile infill, the RSA linear strut is calibrated with an equivalent secant stiffness at 1% interstorey drift, according to Bolis et al. (2017). For the PO and NLTH, the infill macro-model accounts for a multilinear cyclic response as a result of the combination of three parallel non-linear axial springs, calibrated on the analytical prediction of the infill response validated against experimental tests (Pelucco, 2024).

The PO and NLTH models adopts the fiber modelling approach from Spacone et al. (1996) for the RC elements. Beams and columns adopt a refined discretization strategy to capture inelastic behaviour and varying confinement effects. Columns are divided into three regions: two end zones with confined concrete properties with inelastic deformation and a central unconfined elastic zone. Plastic hinge formation is captured using Lobatto integration with two Gauss points at each end, in line with the method proposed by Ghannoum, & Moehle, (2012), while the central region is modelled with five integration points. The yield penetration of reinforcement in the foundation and in the column joint is taken into account by non-linear zero-length element calibrated to simulate rebar extension into adjoining members. A similar strategy is applied to beams, where the central region is modelled as elastic with a reduced moment of inertia by a factor of 0.35 to account for cracking, following Paulay & Priestley, (1992).

Beam-column joints are modelled implicitly by extending beam and column elements into the joint region. On the beam side, an elastic extension with reduced stiffness representing cracked sections is used, while no reduction is applied on the column side.

Geometric nonlinearity is considered in the structural model through the inclusion of P-Delta effects, ensuring accurate representation of second-order moments under lateral seismic loading. The complete modelling scheme is summarised schematically in Fig. 3.

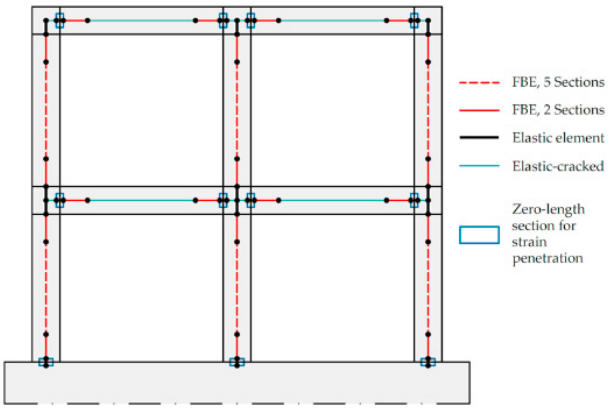

Fig. 3. Modelling scheme represented for a two-bay and two-storey frame (“FBE” = Force based element, “5 Sections” = 5 integration sections assumed for the element, “2 Sections” = 2 integration sections assumed for the element, “Elastic-cracked” = Elastic element characterised by sectional stiffness reduced to 35% of the uncracked section) (Pelucco, 2024).

The capacity of the structure for the different limit state is defined at both global and local levels. Specifically, for the Near Collapse Limit State (NC), at the local level, collapse occurs when either the confined concrete reaches its ultimate compressive strain or the reinforcing steel reaches 4.00% tensile strain, as captured directly through the fibre-

based model. Shear failure is not explicitly assessed, based on previous findings (Pelucco, 2024) which showed that adequate stirrup detailing can mitigate the shear demands introduced by infills. Globally, NC is identified by either a 15% drop in lateral resistance or exceeding a 4.0% interstorey drift, consistent with NIST GCR 17-917-46v3 guidelines and supported by experimental evidence from Preti et al. (2015) and Morandi et al. (2018). The Significant Damage Limit State (SD) is defined by limiting material strains to 75% of those at NC and by adopting 1.5% and 2.5% interstorey drift thresholds for traditional and ductile masonry infills respectively. The value for ductile infill is based on the same experimental studies, which showed infill systems maintaining integrity up to 3.0% drift. For lower damage states, interstorey drift limits of 0.5% for the Operational Performance Limit State (OP) and 1.25% for the Damage Limitation Limit State (DL) are adopted for ductile infills, reduced to 0.2% and 0.5% respectively for traditional infills.

The design demand for the four limit state is quantified using the N2 method Fajfar & Gašperšič, (1996) for the PO, while seven spectrum-compatible accelerograms are adopted for NLTH, as detailed in Table 3.

Table 3. Selected ground motions for SD.

Code	Recorder ID	ID ITACA	Scale factor
SD1	IT.NOR.00.HG.EMSC-20161026_0000077	EMSC-	E: 2.210
SD2	IT.MTR.00.HG.EMSC-20160824_0000006	EMSC-	E: 4.395
SD3	IT.SAN0.00.HN.IT-2012-0011	IT-2012-0011	N: 1.605
SD4	IT.MRN.00.HN.IT-2012-0008	IT-2012-0008	E: 1.352
SD5	IT.SAN0.00.HN.IT-2012-0011	IT-2012-0011	E: 2.035
SD6	IT.NOR.00.HG.EMSC-20161026_0000095	EMSC-	N: 2.939
SD7	IV.T0819..HN.IT-2012-0010	IT-2012-0010	E: 1.374

4. Numerical results

This section presents key findings from the parametric analysis, focusing on the seismic performance of bare and infilled frame configurations designed for high ductility. These results were obtained using the three analysis methods performed, which are RSA, modal PO, and NLTH analysis, as shown in Fig. 4. The comparison in Fig. 4(a) highlights that RSA and modal PO results are in good agreement with each other, and also NLTH, though discrepancies occur at upper floors. A better match is observed in infilled frames compared to the bare one for both interstorey drift and displacement. Furthermore, RSA offers a safe estimate of the maximum interstorey drift and top displacement. To further evaluate the accuracy of linear and nonlinear analyses, Fig. 4(b) compares maximum interstorey drift demands at the NC limit state, highlighting deviations of RSA and PO from NLTH across different infill thicknesses and ductility levels. Infilled configurations consistently show lower deviation (under 20%) compared to bare frame. RSA results closely align with those of PO. Overall, both RSA and modal PO demonstrate a good ability to approximate NLTH demands.

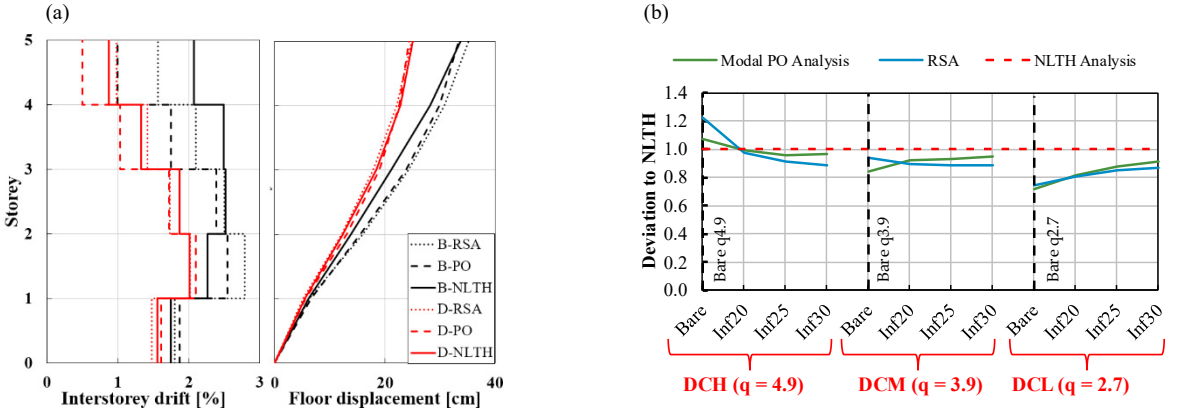

Fig. 4. (a) Comparison of interstorey drift and displacement demand profiles at the Life Safety (LS) limit state from modal PO, RSA, and NLTH analyses for bare and ductile infilled frames (B: Bare frame, D: Ductile infill frame). (b) Relative deviation of interstorey drift demands from modal PO and RSA analyses compared to NLTH results at the Near Collapse (NC) limit state.

Fig. 5 compares capacity and demand in the force-displacement response for bare and infilled high-ductility frames, as quantified by the PO assuming a distribution of acceleration at the floor levels consistent with the frame in the 1st mode of vibration (modal PO). For comparison, the same frame with non-ductile infills ("traditional," i.e., having the same masonry properties as the ductile one but with a continuous running bond layout across the entire bay span) is also included. The corresponding nonlinear frame deformation mechanisms at the NC limit state are shown in Fig. 6. Fig. 5 indicates that the bare and ductile infilled frames show a similar hardening response shapes, but the ductile infilled frame exhibits higher initial stiffness and overall lateral strength. The traditional infilled frame shows the highest initial stiffness and peak strength, followed by a degradation of more than 15%. Among the three configurations, only the ductile infill configuration meets the displacement demands for all limit states. As shown in Fig. 6, the presence of ductile infills does not significantly alter the mechanism at the NC limit state from the bare to ductile infilled case. In the traditional infilled frame, a soft-storey mechanism develops at the 1st and 2nd storeys, which is not observed in either the bare or ductile infilled frames.

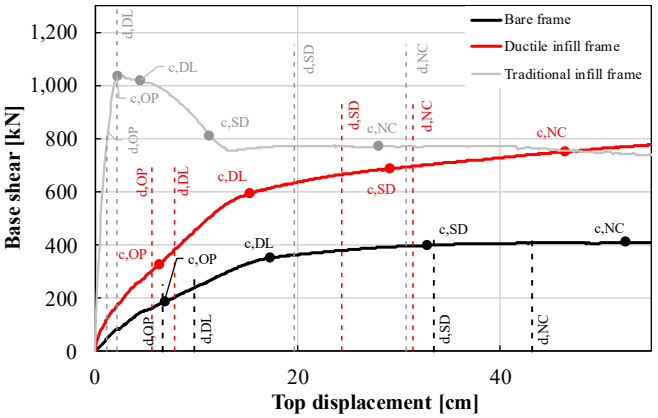

Fig. 5. Comparison of capacity curves with demands from modal PO analysis for bare, traditional and ductile infilled frames.

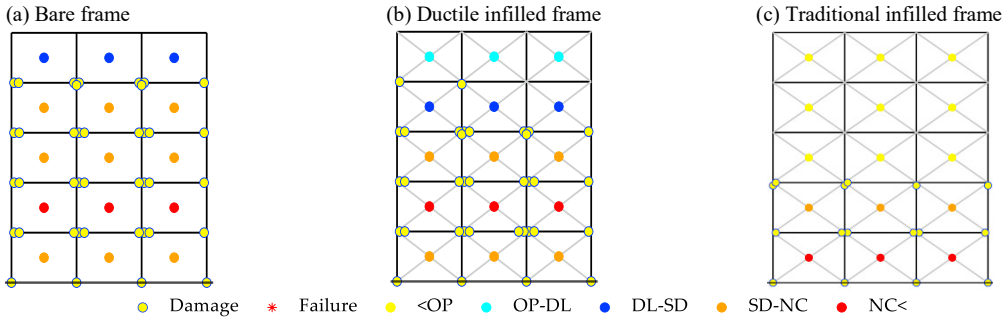

Fig. 6. Comparison of the mechanisms at the NC limit state capacity for (a) bare, (b) ductile, and (c) traditional infilled frames under modal PO analysis. For the beam, two control sections are considered: one at the beam-column interface, and another located at a distance equal to the critical length from the same beam end section.

Extending the investigation, Fig. 7 and Fig. 8 examine the effects of non-regularity in elevation of the infill distribution, specifically analysing a soft ground storey layout. The force-displacement curves and nonlinear deformation mechanisms are compared for two configurations: a frame designed without accounting for this non-regularity, and one in which the soft storey is strengthened according to the criterion proposed in Eurocode 8 (2004) §4.3.6.3.2. Strengthening is applied by amplifying the seismic design action in the columns of the soft storey using the factor η, defined in Equation 1.

$$\eta = (1 + \Delta V_{Rw}/\Sigma V_{Ed}) \tag{1}$$

where, ΔV_{Rw} is the total reduction of the resistance of infills in the storey concerned, compared to the more infilled storey above, and ΣV_{Ed} is the sum of the seismic shear forces acting on all vertical primary seismic members of that storey.

Due to the absence of infill at the ground storey, a soft-storey mechanism develops at this level, more pronounced in the traditional infilled case, as shown in Fig. 7, indicating the need for column strengthening. When strengthening is applied, the soft-storey mechanism develops at the storey above in the traditional configuration but is not observed in the ductile infilled case. Fig. 8 compares the capacity curves of these configurations. Lateral strength resistance increases in both strengthened cases, though to a lesser extent for ductile infills. The curve shape remains similar in the ductile infill cases but changes for traditional infills. The required increase in strength is approximately 30% for the ductile infill and 70% for the traditional infill configuration. For the ductile infill, strengthening is achieved by simply increasing the column reinforcement ratio, whereas for the traditional infill, an increase in the column cross-section is also required.

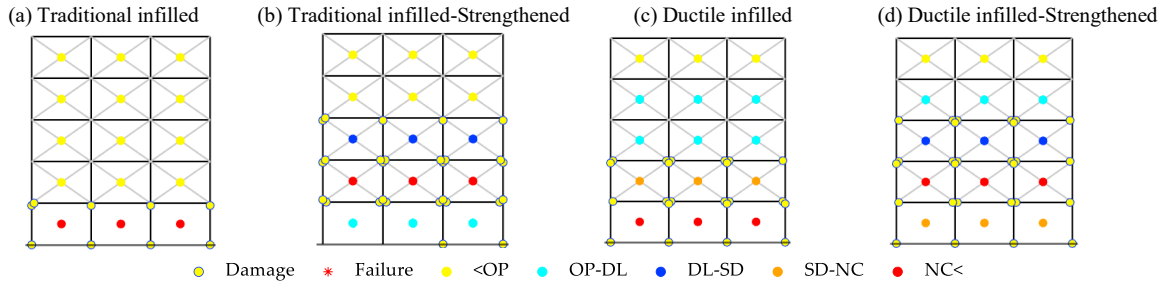

Fig. 7. Comparison of mechanisms at the capacity NC limit state for (a)(b) traditional, and (c)(d)ductile infilled frames without first-storey infill.

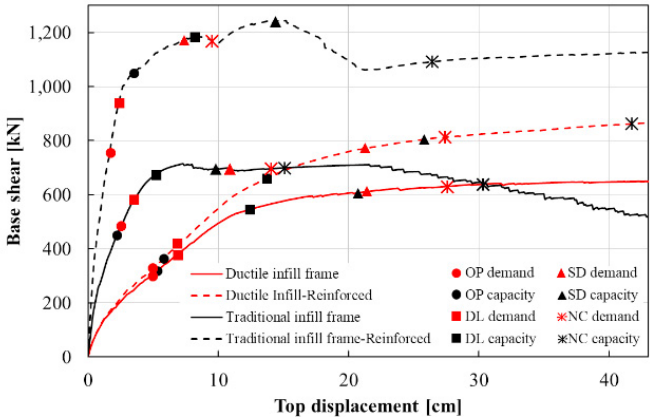

Fig. 8. Comparison of capacity curves with demands from mass PO analysis for traditional, and ductile infilled frames without first-storey infill.

5. Conclusions

The first results of a parametric analysis focusing on the effect of ductile infills in a reinforced concrete frame are presented in the paper. The presented results suggest the following trend:

- Simplified analyses such as linear dynamic analysis or non-linear static analysis seem to well capture the response obtained by means of more refined non-linear time history analyses;
- The ductile infills seem not to alter the non-linear response of RC frames designed for ductility. No concentration of the infill damage and deformation at a single storey is observed, which is otherwise observed in traditionally infilled frames (induced soft story mechanism);
- Non regular distribution of infills in elevation is observed to cause story drift concentration in both traditional and ductile infills. However, the global response in presence of ductile infills remained ductile and the drift concentration is less pronounced;

- Mitigation of story infill reduction by local strengthening of vertical primary resisting elements at the weak story was tested, following the Eurocode 8 (2004) approach. In both cases, the strengthening mitigated the soft-story mechanism. However, the required strengthening in the two cases is very different, resulting in a 70% increase in lateral force strength for traditional infills versus 30% when adopting ductile infills.

Those results are promising in reducing the post-earthquake damage and simplifying the seismic design of infilled RC structures. However, further analyses and results for different case studies are still needed to confirm the findings.

Acknowledgements

The study presented in this work has been supported within the framework of DPC/ReLUIS project 2022-2024, WP10. A special thanks to Ph.D. Valentino Bolis who contributed to build the knowledge of the author on this topic in a fruitful ten year collaboration.

References

Applied Technology Council. (2017). Guidelines for nonlinear structural analysis and design of buildings. Part IIb—Reinforced concrete moment frames (No. NIST GCR 17-917-46v3; p. NIST GCR 17-917-46v3). National Institute of Standards and Technology. https://doi.org/10.6028/NIST.GCR.17-917-46v3

Bolis, V., Stavridis, A., & Preti, M. (2017). Numerical Investigation of the In-Plane Performance of Masonry-Infilled RC Frames with Sliding Subpanels. Journal of Structural Engineering, 143(2), 04016168. https://doi.org/10.1061/(ASCE)ST.1943-541X.0001651

Braga, F., Manfredi, V., Masi, A., Salvatori, A., & Vona, M. (2011). Performance of non-structural elements in RC buildings during the L'Aquila, 2009 earthquake. Bulletin of Earthquake Engineering, 9(1), 307–324. https://doi.org/10.1007/s10518-010-9205-7

Di Trapani, F., Bolis, V., Basone, F., & Preti, M. (2020). Seismic reliability and loss assessment of RC frame structures with traditional and innovative masonry infills. Engineering Structures, 208, 110306. https://doi.org/10.1016/j.engstruct.2020.110306

DM 17 gennaio 2018— NTC. Ministry Decree, Norme tecniche per le costruzioni (Technical codes for construction) [in Italian]; 2018.

Eurocode 8: Design of structures for earthquake resistance - Part 1: general rules, seismic actions and rules for buildings. European Committee for Standardization, Brussels; 2004.

Fajfar, P., & Gašperšič, P. (1996). THE N2 METHOD FOR THE SEISMIC DAMAGE ANALYSIS OF RC BUILDINGS. Earthquake Engineering & Structural Dynamics, 25(1), 31–46. https://doi.org/10.1002/(SICI)1096-9845(199601)25:1<31::AID-EQE534>3.0.CO;2-V

Fikri, R., Dizhur, D., Walsh, K., & Ingham, J. (2019). Seismic performance of Reinforced Concrete Frame with Masonry Infill buildings in the 2010/2011 Canterbury, New Zealand earthquakes. Bulletin of Earthquake Engineering, 17(2), 737–757. https://doi.org/10.1007/s10518-018-0476-8

Final Draft EN1998–1–2 NEN SC8 PT2 2019b–11–08 Draft Eurocode 8: Design of structures for earthquake resistance—Part 1–2: Rules for new buildings. 2019. (n.d.).

Ghannoum, & Moehle. (2012). Dynamic Collapse Analysis of a Concrete Frame Sustaining Column Axial Failures. Aci Structural Journal, 109(3), 403–412. https://doi.org/10.14359/51683754

Ju, R.-S., Lee, H.-J., Chen, C.-C., & Tao, C.-C. (2012). Experimental study on separating reinforced concrete infill walls from steel moment frames. Journal of Constructional Steel Research, 71, 119–128. https://doi.org/10.1016/j.jcsr.2011.10.004

Langenbach, R. (2007). From "Opus Craticium" to the "Chicago Frame": Earthquake-Resistant Traditional Construction∗. International Journal of Architectural Heritage, 1(1), 29–59. https://doi.org/10.1080/15583050601125998

Mohammadi, M., & Akrami, V. (2010). An engineered infilled frame: Behavior and calibration. Journal of Constructional Steel Research, 66(6), 842–849. https://doi.org/10.1016/j.jcsr.2010.01.008

Morandi, P., Milanesi, R. R., & Magenes, G. (2018). Innovative solution for seismic-resistant masonry infills with sliding joints: In-plane experimental performance. Engineering Structures, 176, 719–733. https://doi.org/10.1016/j.engstruct.2018.09.018

Paulay, & Priestley. (1992). Seismic Design of Reinforced Concrete and Masonry Buildings.

Pelucco, S. (2024). Seismic performance and modelling of reinforced concrete frames infilled with horizontal sliding joint deformable infills [PhD thesis]. Università degli Studi di Brescia.

Preti, M., Bettini ,N., & and Plizzari, G. (2012). Infill Walls with Sliding Joints to Limit Infill-Frame Seismic Interaction: Large-Scale Experimental Test. Journal of Earthquake Engineering, 16(1), 125–141. https://doi.org/10.1080/13632469.2011.579815

Preti, M., Bolis ,V., & and Stavridis, A. (2019). Seismic infill–frame interaction of masonry walls partitioned with horizontal sliding joints: Analysis and simplified modeling. Journal of Earthquake Engineering, 23(10), 1651–1677. https://doi.org/10.1080/13632469.2017.1387195

Preti, M., Migliorati, L., & Giuriani, E. P. (2015). Experimental testing of engineered masonry infill walls for post-earthquake structural damage control. https://doi.org/10.1007/s10518-014-9701-2

Spacone, E., Filippou, F. C., & Taucer, F. F. (1996). Fibre Beam–Column Model for Non-Linear Analysis of R/C Frames: Part I. Formulation. Earthquake Engineering & Structural Dynamics, 25(7), 711–725. https://doi.org/10.1002/(SICI)1096-9845(199607)25:7<711::AID-EQE576>3.0.CO;2-9